A Near-Vertical Slab Tear in the Southeastern Solomon Islands

Ching-Yu Cheng[1], Hao Kuo-Chen[2], Dennis Brown[3], Wei-Fang Sun[2], Chin-Shang Ku[4], Yu-Ting Kuo[5], Bor-Shouh Huang[6], and Yue-Gau Chen[7]

[1]National Central University
[2]National Taiwan University
[3]Geosciences Barcelona, CSIC
[4]Academia Sinica
[5]National Chung Cheng University
[6]Institute of Earth Sciences, Academia Sinica, Taiwan
[7]Research Center for Environmental Changes Academia Sinica

August 4, 2023

Abstract

The southeastern part of the Solomon Islands, a highly seismically active area in the southern Pacific, experienced two moderate earthquakes (Mw 6.3 and 6.0) on January 27th and 29th, 2020. The regional seismic network, operational since October 2018, recorded the entire foreshock-main-shock-aftershock sequence, allowing for a new 1D velocity model and relocation of events. Based on the spacial distribution of the foreshock-aftershock sequence, together with focal mechanism data from the Global CMT database, we suggest that there is a near-vertical slab tear at the southern end of the South Solomon subducting slab, abutting a zone of strike-slip faulting that links it to the Vanuatu subduction zone to form a Subduction-Transform Edge Propagator fault. Our new data also indicates that a seismic gap occurs at depths from 25 to 35 km within the southern part of the South Solomon slab.

A Near-Vertical Slab Tear in the Southeastern Solomon Islands

C.-Y. Cheng[1*], H. Kuo-Chen[2], D. Brown[3], W.F. Sun[2], C.-S. Ku[4], Y.-T. Kuo[5], B.-S. Huang[4], and Y.-G. Chen[6]

[1]Department of Earth Sciences, National Central University, Taoyuan 320, Taiwan.
[2]Department of Geosciences, National Taiwan University, Taipei 10617, Taiwan.
[3]Geosciences Barcelona, CSIC, 08028 Barcelona, Spain.
[4]Institute of Earth Sciences, Academia Sinica, Taipei 11529, Taiwan.
[5]Department of Earth and Environmental Sciences, National Chung Cheng University, Chiayi 621301, Taiwan.
[6]Research Center for Environmental Changes, Academia Sinica, Taipei 11529, Taiwan.

Corresponding author: Ching-Yu Cheng (doll3219@gmail.com)

Abstract

The southeastern part of the Solomon Islands, a highly seismically active area in the southern Pacific, experienced two moderate earthquakes (Mw 6.3 and 6.0) on January 27th and 29th, 2020. The regional seismic network, operational since October 2018, recorded the entire foreshock-main-shock-aftershock sequence, allowing for a new 1D velocity model and relocation of events. Based on the spacial distribution of the foreshock-aftershock sequence, together with focal mechanism data from the Global CMT database, we suggest that there is a near-vertical slab tear at the southern end of the South Solomon subducting slab, abutting a zone of strike-slip faulting that links it to the Vanuatu subduction zone to form a Subduction-Transform Edge Propagator fault. Our new data also indicates that a seismic gap occurs at depths from 25 to 35 km within the southern part of the South Solomon slab.

Plain Language Summary

In October, 2018, a new regional seismic network was established in the southeastern Solomon Islands with six broadband seismic stations. In January, 2020, two large earthquakes occurred in the southeastern part of the Solomon Islands. The entire foreshock-aftershock sequence was recorded by the new network. Since a good 1D local velocity model is crucial for determining earthquake locations, we use the data set from this earthquake sequence to calculate a new 1D velocity model, and compare the earthquake hypocenter locations with those determined using the Preliminary Reference Earth Model (PREM). After the earthquakes are reliably located, we use the distribution of the foreshock-aftershock hypocenters to investigate the seismogenic structures in the southeastern South Solomon subduction zone and its link with the Vanuatu subduction zone. On the basis of these results, we suggest that there is a near-vertical slab tear along what we call the Makira – Santa Cruz transform forming what is termed a subduction-transform edge propagator (STEP) fault. We also observe a seismic gap in the South Solomon slab at depths from 25 to 35 km that is observed for the first time. With the current data set, the significance of this seismic gap is unclear.

1 Introduction

Extending for ~300 km in length, the link between the southeastern part of the South Solomon subduction zone and the northwestern Vanuatu subduction zone (Fig. 1) has been variably interpreted to be a subduction to strike-slip transition zone (e.g., Bilich et al., 2001) or has a continuation of the San Cristobal subduction zone but with a shortened slab length and a tear in the vicinity of the Santa Cruz Islands, where it interacts with the Vanuatu slab (e.g., Richards et al., 2011; Holm et al., 2016). Previous studies have mainly focused on the tectonic evolution of the Solomon Islands (e.g., Yan and Kroenke, 1993; Mann et al., 1998; Petterson et al., 1999; Mann and Taira, 2004; Holm et al., 2016), their geology (e.g., Mann et al., 1998; Taylor et al., 2005; Taylor et al., 2008; Chen et al., 2011), regional seismology (e.g., Cooper and Taylor, 1985; Mann and Taira, 2004; Chen et al., 2011), and crustal and upper mantle structures using ocean-bottom seismometer data (e.g., Mann et al., 1996; Phinney et al.,1999; Mann and Taira, 2004; Miura et al., 2004). To date, the subduction zone in the southeastern Solomon Islands and its possible linkage with the Vanuatu subduction zone has not been documented in detail due to sparse coverage of the area by seismic stations that could provide a data set with sufficient resolution for investigating the complex seismogenic, crustal, and upper mantle structures.

On January 27 and 29, 2020, two moderate earthquakes, Mw 6.3 and Mw 6.0, respectively, occurred in the southeastern Solomon Islands. The entire foreshock-main-shock-aftershock sequence was recorded by a new regional-scale seismic network that was set up in 2018. The earthquake sequence was located in the southeastern end of the South Solomon subduction zone, abutting the linkage zone with the Vanuatu subduction zone, providing a unique opportunity to look into the crustal and upper mantle structures of this tectonically complex region. The aim of this paper is to first derive a new, optimized local 1D P-wave velocity model utilizing the complete earthquake sequence, and compare the relocated hypocenters with those located using the Preliminary Reference Earth Model (PREM) (Dziewonski and Anderson, 1981). We then investigate the implications of the hypocenter locations for the structure of the southeastern part of the South Solomon subdction zone and its linkage with the Vanuatu subduction zone.

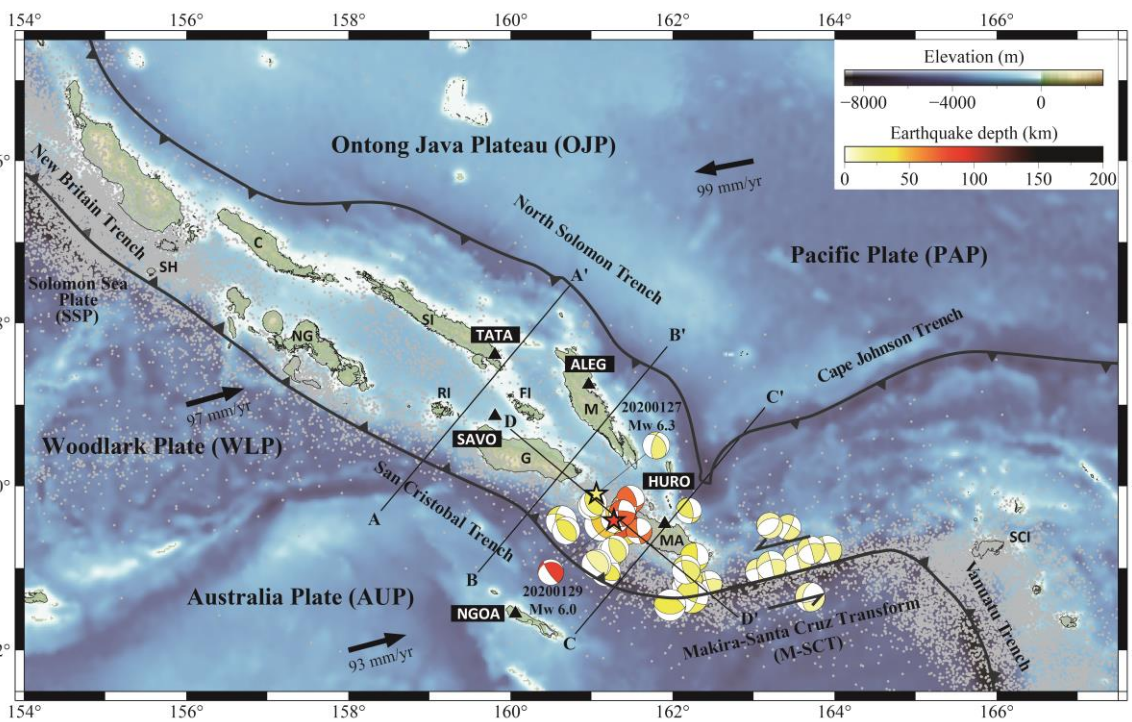

Figure 1. Topography, bathymetry, and regional tectonic setting of the Solomon Islands region. Arrows indicate direction and rate of plate motion of the Australia, Pacific, and Woodlark plates (NUVEL-1A, Demets et al., 1994); heavy lines with triangles represent subduction boundaries; black triangles are broadband seismic stations; two stars in the southeastern Solomon Islands

represent earthquakes occurred on January 27 and 29 from the Incorporated Research Institutions for Seismology (IRIS) catalog; focal mechanisms color-coded by depth are from GCMT; background seismicity are shown as gray dots and are compiled by the IRIS event catalog for the period 1971-2021; AA’, BB’, CC’ and DD’ are the cross sections in Figs. 2 and 4. SH, Shortland Islands; C, Choiseul; NG, New Georgia Island Group; SI, Santa Isabel; RI, Russell Islands; FI, Florida Islands; G, Guadalcanal; M, Malaita; MA, Makira; SCI, Santa Cruz Islands.

2 Tectonic setting

The Solomon Islands is located in a complex and active plate boundary where involving interactions among the Pacific plate (PAP), the Australian plate (AUP), and the associated microplates (i.e., the Woodlark plate and Solomon Sea plate) (Fig. 1) (e.g., Demets et al., 1990, 1994, 2010; Beavan et al., 2002; Miura et al., 2004; Phinney et al., 2004; Taira et al., 2004; Taylor et al., 2005, 2008; Argus et al., 2011; Newman et al., 2011). In the southern Solomon Islands, the Woodlark plate and the AUP subduct beneath the PAP forming the New Britain Trench, San Cristobal Trench and Vanuatu Trench (e.g., Taylor and Exon, 1987; Crook and Taylor, 1994; Taylor et al., 1995; Mann et al., 1998; Taylor et al., 2005). Using data from global seismic networks, previous seismological investigations suggest that active subduction now occurs primarily in the southeastern part of the South Solomon subduction zone, along the San Cristobal Trench (e.g., Cooper and Taylor, 1987; Mann et al., 1998; Chen et al., 2011). Furthermore, there is a waning, southwestward subduction of the Ontong Java Plateau along the North Solomon subduction zone, albeit with slight convergence (e.g., Taylor and Exon, 1987; Yan and Kroenke, 1993; Crook and Taylor, 1994; Mann et al., 1998; Petterson et al., 1999; Mann and Taira, 2004). The Solomon arc is considered a representative example of an island arc polarity reversal due to its unique opposing, double subduction zone setting.

The region around Makira Island and the Santa Cruz Islands (Fig. 1) contains two subduction-to-strike-slip transition (SSST) regions and a transform fault system linking the South Solomon and Vanuatu subduction zones (Bilich et al., 2001). In what follows, we call this the Makira-Santa Cruz transform (M-SCT). Although seismicity indicates a strike-slip motion along this zone (Fig. 1), some studies propose that the South Solomon slab may continues eastward along it, though significantly shortened, until it tears at the beginning of the Vanuatu subduction zone near the western end of the Santa Cruz Islands (Mann and Taira, 2004; Richards et al., 2011; Holm et al., 2016). The aim of this paper is to investigate the nature of the transition from the South Solomon subduction zone to the Makira-Santa Cruz transform.

3 Seismic network and data processing

In October, 2018, the Institute of Geological and Nuclear Sciences Limited (GNS), New Zealand, deployed six permanent seismic stations in different islets of the southeastern Solomon Islands (Fig. 1). To date, this seismic network has been maintained by the Ministry of Mines, Energy and Rural Electrification of the Solomon Islands Government. The instruments are equipped with broadband seismometer (Trillium 120PA; Nanometrics Inc., Canada) and 24-bits digital recorder (Q330S; Quanterra Inc., U.S.A.) with sampling rates of 100 Hz. Except for a timing problem with station LUES, most of the seismic waveforms recorded by the other five stations have good signal-to-noise ratios.

In this study, we processed two-month of continuous seismic waveforms from the GNS network, covering one month before and after the two January, 2020 events, encompassing the entire foreshock-aftershock earthquake sequence. In total, 730 earthquakes (Fig. 2a) were listed in the preliminary catalog, of which 651 were located within the seismic network. The data set is formatted with the daily miniSEED and we used the SeisAn Earthquake analysis software (SEISAN) to establish the event database (Havskov and Ottemoller, 1999). Most of the events occurred close to the seismic network, so we were able to extract numerous high-quality seismic waveforms to pick P- and S-wave arrivals, locate earthquakes and determine magnitudes. The earthquake catalog contains events detected by at least three stations and has more than one clear S-wave arrival to effectively constrain the depths of earthquakes. The interpolated 1D PREM velocity model was used as the reference model to locate earthquake hypocenters. We located earthquakes by the HYPOCENTER program (e.g., Lienert et al., 1986) and determined moment magnitude (M_w) by spectral analysis (e.g., Havskov and Ottemoller, 2010). Following this, we then used the program VELEST (Kissling, 1988, Kissling et al., 1994) to derive a new 1D velocity model, which produces the smallest possible uniform error for a set of seismic events with well-constrained locations. For this new velocity model, only events within the range of the seismic network with the root-mean-square error in arrival time from 0.5 to 1.0 s were used to invert a new

1D velocity model. In total, 389 events were selected for inversion to derive the preferred 1D model and then with it we relocated all 730 earthquakes to obtain the final catalog.

4 Results

4.1. New 1D velocity model

Because the initial velocity model (i.e. PREM) plays a crucial role in accurately locating earthquakes (Fig. 2b), it is important to determine the uncertainities involved. For the PREM velocity model, we calculate the standard error of the means in vertical (ERZ) and horizontal (ERH) as well as the root-mean-square error in arrival time of the 730 event locations in our data set to be 24.7 $\pm$ 19.15 km, 13.43 $\pm$ 10.8 km, and 0.61 $\pm$ 0.30 s, respectively. The moment magnitudes (M_w) determined in this study mostly range from 2.0 to 4.0 with a maximum of 4.9. For the new velocity model, the calculated root-mean-square error in arrival time is 0.66 $\pm$ 0.30 s. The distribution of the root-mean-square error in arrival times are more centralized after relocating and this may indicate the new model (Fig. 2b) is closer to the actual observed arrival times for this region. Furthermore, in comparison with PREM, the new velocity model has a higher velocity layer between 10 km and 25 km depth and slower velocity from 25-35 km depth (Fig. 2). At shallow depth (~10 km) the hypocenters relocated by the new velocity model are deeper and the cluster is more concentrated (Fig. 2c). At greater depth, the cluster becomes more concentrated.

4.2. South Solomon seismicity

In map view, our January-to-February 2020 data set reveals a significant rise in earthquake occurrences in the southeast. The majority of hypocenters form a single cluster, deepening northward near Makira Island, at the boundary between the South Solomon subduction zone and the Makira – Santa Cruz transform (Fig. 3). Other events form small clusters, or dispersed single events that extend from Santa Isabel Island and along the Makira - Santa Cruz transform. In the southeast, the South Solomon subduction zone hypocenters can be broadly divided into two clusters; a shallow cluster at roughly 0 to 25 km depth, and a second cluster between about 50 km and 100 km depth (Figs. 4a, b, and c). It is not clear from this data set whether the deeper events (>100 km) around Santa Isabel and Malaita islands (Fig. 3) are related to the South or North

Solomon subduction zones. Nevertheless, the hypocenters suggest that the South Solomon slab steepens significantly southeastward, from about 45^{o} near Santa Isabel Island to around 80^{o} at the transition to the Makira – Santa Cruz transform (Fig. 4). The area of shallow to moderately deep (ca. 100 km) earthquakes that form an open cluster between Santa Isabel and Malaita islands are clearly related to the North Solomon subduction zone (Fig. 4a). The amount of seismicity that can be attributed to the North Solomon subduction zone decreases significantly toward the southeast. In cross section, hypocenter locations suggest that the North Solomon slab dips about 60^{o}. In a NW-SE section, seismicity related to the North Solomon subduction zone decreases and shallows significantly at the Makira – Santa Cruz transform (Fig. 4d).

To gain further insight into the South Solomon subduction zone and its transition into the Makira – Santa Cruz transform, we also look at the background seismicity from 1971 to 2021 recorded in the IRIS catalog (Figs. 1 and 4). In these 50 years, ca. 5100 events were recorded in our study area. Overall, these show the same trends as our data set (Figs. 4e, f, g, and h), and this allows us to more confidently the interpret deeper (>100 km) events around Santa Isabel and Malaita islands to be related to the North Solomon subduction zone, whose slab appears to extend southward beneath that of the South Solomon subduction zone (Fig. 4e). The background seismicity also indicates that the South Solomon slab steepens towards the southeast. In a NW-SE section, it also shows that seismicity related to the North Solomon subduction zone decreases and shallows significantly at the Makira – Santa Cruz transform (Fig. 4h).

With only five active stations, it is not possible to determine focal mechanisms with our network. Nevertheless, focal mechanisms extracted from the Global CMT database shows the two January, 2020 main shocks to be oblique thrusts, similar to other events of MW >6.0 that occurred between 2000 and 2023 (Fig. 1). Along the Makira – Santa Cruz transform, focal mechanisms are nearly all strike-slip.

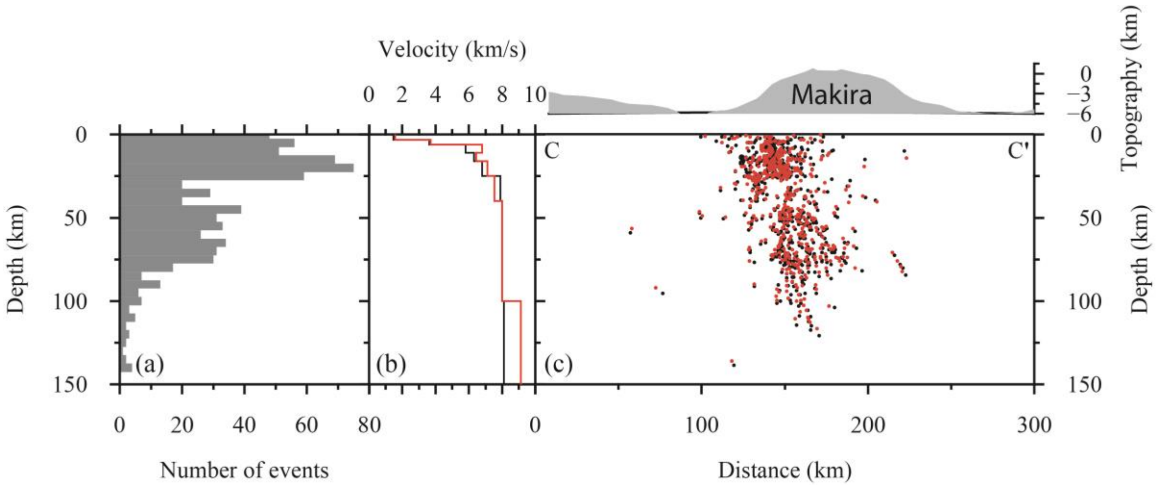

Figure 2. Seismic cluster of the southeastern Solomon Islands. (a) The event distribution in 5 km depth intervals. (b) The 1D interpolated PREM (black line) and the new velocity model (red line). Note the seismic gap between 25 km and 35 km depths. (c) CC' cross section (in Fig. 4) with the seismic cluster located by the reference model (black dots) and relocated by the new velocity model (red dots).

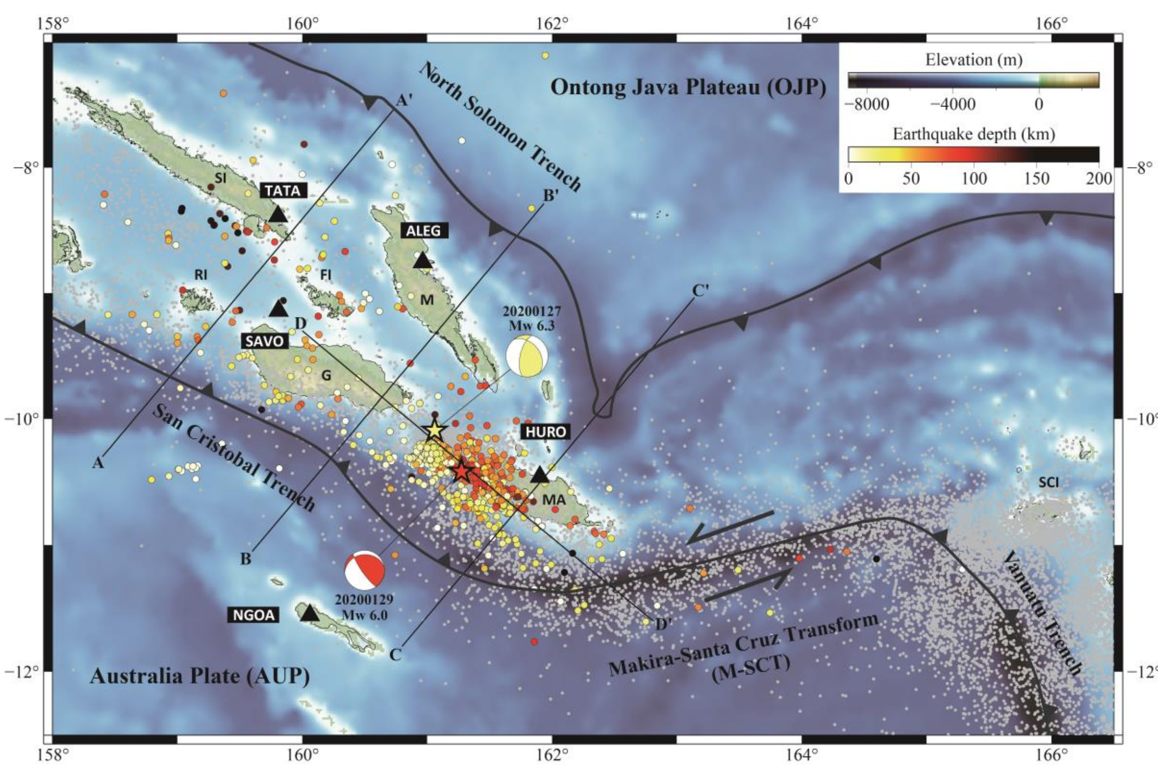

Figure 3. The spacial distribution of the foreshock-aftershock sequence. Topography, bathymetry, regional tectonic setting, and background seismicity are the same as in Fig. 1; circles color-coded by depth indicate foreshocks and aftershocks recorded by GNS seismic stations; stars are locations of the two January, 2020 main shocks; focal mechanisms of two main shocks are from GCMT and color-coded with depth.

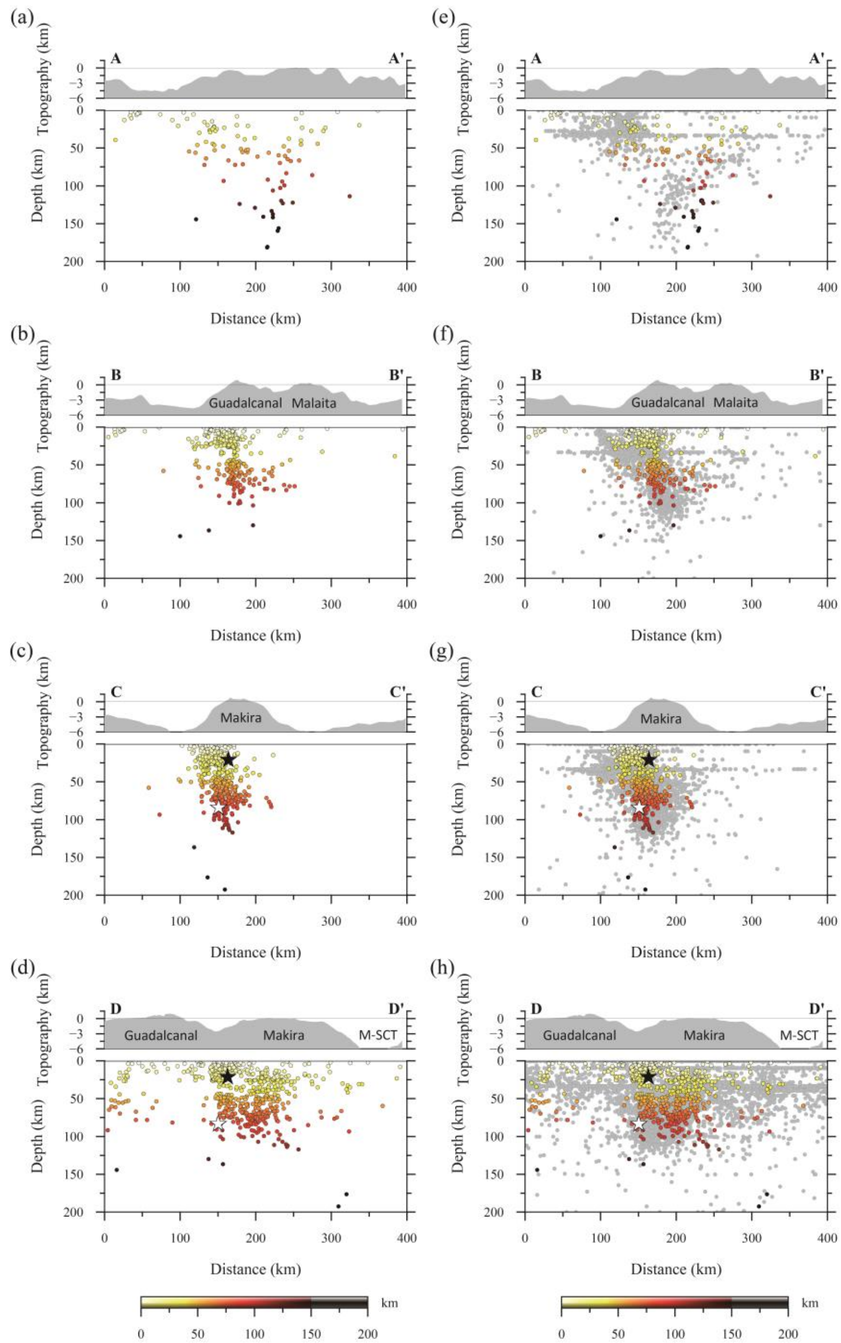

Figure 4. (a-d) Cross sections of earthquake hypocenters relocated by the new 1D velocity model. Circles color-coded by depth are foreshocks and aftershocks; black and white stars represent January 27 and 29 earthquakes in 2020 from IRIS event catalog; four 200-km-wide project lines are shown in Fig. 1. (e-h) Comparison of earthquake hypocenters located by the new 1D velocity model and background seismicity (gray dots). M-SCT = Makira - Santa Cruz transform.

5 Discussion

We used the complete foreshock-aftershock sequence of the January, 2020 earthquakes, recorded by the new seismic network, to calculate a more detailed 1D velocity model of the crust and mantle in the southeastern Solomon Islands. In particular, compared to PREM our velocity model shows a more varied and higher velocity layer between 10 km and 25 km depth, and a lower velocity from 25 km to 35 km depth where mantle velocities (ca. 8 km/s) are reached (Fig. 2). Recently, Ku et al. (2020) also calculated a low-velocity zone above the Moho in the Western Solomon Islands which they attribute to a lower crustal magma chamber (c.f. Dufek and Bergantz, 2005), but in our study area we unable to assign such a cause for the lower velocities found in our model. Nevertheless, because of the good coverage of the study area provided by the new network, the new velocity model provides better constraints of the quality of the earthquake location results and makes it possible to better locate local, small magnitude earthquakes, even at shallow depths.

STEP faults (or tearing) have been described from a number of subduction zones worldwide (e.g., Bilich et al., 2001; Grovers and Wortel, 2005). For example, Isacks et al. (1969) and Millen and Hamburger (1998) describe tearing along a zone of strike-slip faulting at the northern termination of the Tonga subduction zone, as do Molnar and Sykes (1969) and Clark et al. (2008) for the southern termination of the Lesser Antilles subduction zone. The model for STEP faults developed by Grovers and Wortel (2005), involves a subduction zone terminating at a strike-slip system that can range from 100's to more than a 1000 km in length. Our study area presents a variation on this model in which the STEP fault links two subduction zones and we investigate the termination of the South Solomon subduction zone against the Makira – Santa Cruz transform, or the "convex" SSST of Bilich et al. (2001).

Our results show a steeply inclined seismogenic structure extending from the shallow subsurface to ~120 km depth beneath the island of Makira (Figs. 3 and 4). This structure, along with the background seismicity over the past 50 years, aligns within the SSST at the southwestern end of the Makira – Santa Cruz transform. On the basis of the southeastward truncation of the deep seismicity with predominantly thrust focal mechanisms against the Makira – Santa Cruz transform with predominately strike-slip focal mechanism, we suggest this area forms a subduction-transform edge propagator (STEP) fault (e.g., Grovers and Wortel, 2005) between the South Solomon subduction zone and the Vanuatu subduction zone (Fig. 5). Following the model of Govers and Wortel (2005), we suggest that the subducting South Solomon slab forms a steeply dipping seismogenic structure that terminates against a vertical tear in the lithosphere between the Australian Plate and the end of the Solomon Island arc (Fig. 5). Nevertheless, other authors (e.g., Mann and Taira, 2004; Richards et al., 2011; Holm et al., 2016) have different interpretations of the geometry and location of the southern termination of the South Solomon subduction zone, suggesting that the South Solomon slab continues eastward along the Makira – Santa Cruz transform to a slab tear at the northern termination of the Vanuatu subduction zone. We suggest, however, that geometry of the termination of the South Solomon slab at a STEP fault along the Makira – Santa Cruz transform fits better with the northward deepening seismicity with predominately thrust mechanisms around Makira Island abuting a northeast-trending zone of shallow seismicity with strike-slip mechanisms. In this interpretation, the Makira – Santa Cruz transform has been growing northeastward as the Vanuatu subduction zone advanced in that direction since about 4 Ma ago (e.g., Mann and Taira, 2004; Holm et al., 2016).

Our January-to-February, 2020 data set also suggest a seismic gap at 25-35 km depth within the cluster regardless of whether it is located in the PREM or the new velocity model (Fig. 4). Similar gaps in subduction-related seismicity have also been observed in seismic clusters in the Tonga Trench (Millen and Hamburger, 1998), Gibraltar (Buforn et al., 2004), the southeast Lesser Antilles Trench (Clark et al., 2008), and the northeast Lesser Antilles Trench (Meighan et al., 2013a). There are a few hypotheses regarding the cause of a gap in seismicity. For example, Clark et al. (2008) suggest that the gap images a weak, ductile, lower crustal layer separating a strong upper/middle crustal layer from a strong lithospheric mantle layer, which is interpreted as the "jelly sandwich" rheology (Chen and Molnar, 1983; Watts and Burov, 2003). In this model, Clark et al (2008) interprets the subducting slab to be detached from the buoyant South American plate along a near-vertical tear in the southeast corner of the Lesser Antilles Trench. Meighan et al. (2013b), propose that in the northeast Lesser Antilles subduction termination that the slab is overlain by an aseismic mantle wedge (e.g., van Keken et al., 2011), and therefore not directly contact with the overlying arc crust. In this model, the seismic gap is because there is shallow seismicity in the arc, no seismicity in the ductile mantle wedge, and then a vertical band of seismicity that crosses the entire slab. From our results, however, it is not clear what the exact reason for the gap in seismicity is. As a preliminary interpretation, we suggest that it could be related to a break in the end of slab that may be related to either drag along the transform and/or an early stage of slab breakoff.

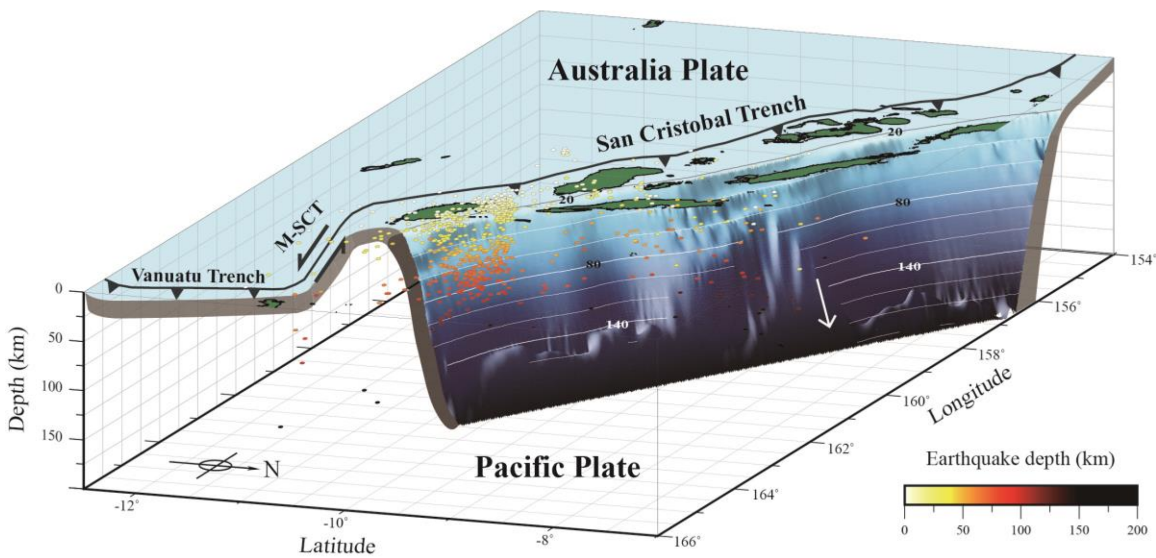

Figure 5. Three-dimensional visualization of the seismic cluster in the southeastern Solomon Islands viewed from northeast. Heavy lines with barbs represent subduction boundaries; solid contour lines are Slab2 – A Comprehensive Subduction Zone Geometry Model (Hayes et al., 2018), contoured every 20 km; earthquake hypocenters show near-vertical slab tear along the Makira – Santa Cruz transform.

6 Conclusions

In this study, we use a new seismic network that was established in the southeastern Solomon Islands in 2018 to provide better quality constraints on locating earthquakes in the area. We used a complete foreshock-aftershock sequence from two Jaunuary, 2020 earthquakes to calculate a new optimized local 1D velocity model and locate the hypocenters. The hypocenters define a steeply dipping earthquake cluster in the region between Makira and Guadalcannal, at the southeastern termination of the South Solomon subductions zone. This cluster terminates against the strike-slip Makira – Santa Cruz transform, which links the South Solomon and Vanuatu subduction zones. We suggest that the geometry and kinematics of this area is that of a thrust-dominated subduction zone termination against a strike-slip dominated subduction-transform edge propagator (STEP) fault. The gap observed in the Makira cluster at depths of 25-35 km may be indicative of a break in the South Solomon slab, although this is not clear from the data set. Futher investigations of the mechanism of slab tear and the cause of the seismic gap will be undertaken in the future.

Acknowledgements

This project is supported by Academic Sinica (Grant NO. AS-TP-110-M02). The assistance from Mr. Douglas Billy and Mr. Carlos Tatapu of Geological Survey Division, Solomon Islands Ministry of Mines, Energy and Rural Electrification (MMERE) are highly appreciated. Kuo-Chen and Brown wish to acknowledge visiting researcher grant NSTC 112-2811-M-002-006.

Open Research

The seismic data set used in this manuscript is available on https://tecdc.earth.sinica.edu.tw/WAV/2020SolomonIs/ (login with Email: solomon@earth.sinica.edu.tw and password: Islands2023).

Maps were created by using Generic Mapping Tools (GMT) version 6 (Wessel et al., 2019).

References

Argus, D. F., R. G. Gordon, and C. DeMets (2011). Geologically current motion of 56 plates relative to the no-net-rotation reference frame, *Geochemistry, Geophysics, Geosystems* **12**, no. 11.

Beavan, J. P., M. Tregoning, M. Bevis, and C. Meertens (2002). Motion and rigidity of the Pacific plate and implications for plate boundary deformation, *J. Geophy. Res.* **107**, 2261.

Bilich A., C. Frohlich, and P. Mann (2001). Global seismicity characteristics of subduction-to-strike-slip transitions, *J. Geophy. Res.* **106**, no. B9, 19433-19452.

Buforn E., M. Bezzeghoud, A. Udías, and C. Pro (2004). Seismic sources on the Iberia-African plate boundary and their tectonic implications, *Pure Appl. Geophys.* **161**, 623-646.

Chen M. C., C. Frohlich, F. W. Taylor, G. Burr, and A. Q. van Ufford (2011). Arc segmentation and seismicity in the Solomon Islands arc, SW Pacific, *Tectonophysics* **507**,47-69.

Chen, W. P., and P. Molnar (1983). Focal depths of intracontinental and intraplate earthquakes and their implications of the thermal and mechanical properties of the lithosphere, *J. Geophys. Res.* **88**, no. B5, 4183-4214.

Clark, S. A., M. Sobiesiak, C. A. Zelt, M. B. Magnani, M. S. Miller, M. J. Bezada, and A. Levander (2008). Identification and tectonic implications of a tear in the South American plate at the southern end of the Lesser Antilles, *Geochemistry, Geophysics, Geosystems* **9**, no. 11.

Cooper, P. A., and B. Taylor (1985). Polarity reversal in the Solomon Islands arc, *Nature* **314**, 428-430.

Cooper, P. A., and B. Taylor (1987). Seismotectonics of New Guinea: a model for arc reversal following arc-continent collision, *Tectonics* **6**, 53-67.

Crook, K., and B. Taylor, (1994). Structure and Quaternary tectonic history of the Woodlark triple junction region, Solomon Islands, *Marine Geophysical Researches* **16**, 65-89.

DeMets, C., R. G. Gordon, and D. F. Argus (2010). Geological current plate motions, *Geophys. J. Int.* **181**, 1-80.

DeMets, C., R. G. Gordon, D. F. Argus, and S. Stein (1990). Current plate motions, *Geophys. J. Int.* **101**,425-478.

DeMets, C., R. G. Gordon, D. F. Argus, and S. Stein (1994). Effect of recent revisions to the geomagnetic reversal time scale on estimates of current plate motions, *Geophys. Res. Lett.* **21**, 2191-2194.

Dufek, J., and G. W. Bergantz (2005). Lower crustal magma genesis and preservation: a stochastic framework for the evaluation of basalt-crust interaction. *J. Petrol.* **46**, 2167–2195.

Dziewonski, A. M., and D. L. Anderson (1981). Preliminary reference Earth model, *Physics of the Earth and Planetary Interiors* **25**(4), 297-356.

Forsyth, D. W. (1975). Fault plane solutions and tectonics of the South Atlantic and Scotia Sea, *J. Geophy. Res.* **80**, no. 11, 1429-1443.

Govers, R., and M. J. R. Wortel1 (2005). Lithosphere tearing at STEP faults: Response to edges of subduction zones, *Earth Planet. Sci. Lett.* **236**, 505-523.

Havskov, J., and L. Ottemoller (1999). SeisAn earthquake analysis software, *Seismol. Res. Lett.*

70, no. 5, 532-534.
Havskov, J., and L. Ottemoller (2010). *Routine Data Processing in Earthquake Seismology*, Springer, Dordrecht, The Netherlands.
Hayes, G. P., G. L. Moore, D. E. Portner, M. Hearne, H. Flamme, M. Furtney, and G. M. Smoczyk (2018). Slab2, a comprehensive subduction zone geometry model, Science **362**, 58-61.
Holm, R. J., G. Rosenbaum, S. W. Richards (2016). Post 8 Ma reconstruction of Papua New Guinea and Solomon Islands: Microplate tectonics in a convergent plate boundary setting, *Earth-Science Reviews* **156**, 66-81.
Isacks, B., L. R. Sykes, and J. Oliver (1969). Focal mechanisms of deep and shallow earthquakes in Tonga-Kermadec region and tectonics of island arcs, *Geol. Soc. Am. Bull.* **80**(8), 1443-1470.
Van Keken, B. E., B. R. Hacker, E. M. Syracuse, and G. A. Abers (2011). Subduction factory: 4. Depth-dependent flux of H_2O from subducting slabs worldwide, *J. Geophys. Res.* **116**, B01401.
Kissling, E. (1988). Geotomography with local earthquake data, *Reviews of Geophysics*. **26**, no. 4,659-698.
Kissling, E., W. L. Ellsworth, D. Eberhart-Phillips, and U. Kradolfer (1994). Initial reference model in local earthquake tomography, *J. Geophy. Res.* **99**, 19635-19646.
Ku, C. S., Y. T. Kuo, B. S. Huang, Y. G. Chen, and Y. M. Wu (2020). Seismic velocity structure beneath the Western Solomon Islands from the joint inversion of receiver functions and surface-wave dispersion curves, *Journal of Asian Earth Science* **195**, 104378.
Lienert, B. R. E., E. Berg, and L. N. Frazer (1986). Hypocenter: An earthquake location method using centered, scaled and adaptively least aquares, *Bull. Seismol. Soc. Am.* **76**, 771-783.
Mann, P., and A. Taira (2004). Global tectonic significance of the Solomon Islands and Ontong Java Plateau convergent zone, *Tectonophysics* **389**, 137-190.
Mann, P., F. W. Taylor, M. B. Lagoe, A. Quarles, and G. Burr (1998). Accelerating late Quaternary uplift of the New Georgia Islands Group (Solomon Island arc) in response to subduction of the recently active Woodlark spreading center and Coleman seamount, *Tectonophysics* **295**, 259-306
Mann, P., M. Coffin, T. Shipley, S. Cowley, E. Phinney, A. Teagan, K. Suyehiro, N. Takahashi, E. Araki, M. Shinohara, S. Miura, and L. Tivuru (1996). Researchers investigate fate of oceanic plateaus at subduction zones, *EOS Transactions American Geophysical Union* **77**, 282-283.

Meighan, H. E., J. Pulliam, U. S. ten Brink, and A. López (2013a). Seismic evidence for a slab tear at the Puerto Rico Trench, *J. Geophys. Res. Solid Earth* **118,** 2915-2923.

Meighan, H. E., U. ten Brink, and J. Pulliam (2013b). Slab tears and intermediate-depth seismicity, *Geophys. Res. Lett.* **40,** 4244-4248.

Millen, D. W., and M. W. Hamburger (1998). Seismological evidence for tearing of the Pacific plate at the termination of the Tonga subduction zone, *Geology* **26**, no. 7, 659-662.

Miura S., K. Suyehiro, M. Shinohara, N. Takahashi, E.Araki, and A. Taira (2004). Seismological structure and implications of collision between the Ontong Java Plateau and Solomon Island Arc from ocean bottom seismometer-airgun data, *Tectonophysics* **389**, 191-220.

Molnar, P., and L. R. Sykes (1969). Tectonics of the Caribbean and Middle America region from focal mechanisms and seismicity, *Geol. Soc. Amer. Bull*. **80**, 1639.

Newman, A. V., L. J. Feng, H. M. Fritz, Z. M. Lifton, N. Kalligeris, and Y. Wei (2011). The energetic 2010 M_W 7.1 Solomon Islands tsunami earthquake, *Geophys. J. Int.* **186**, 775-781.

Petterson, M., T. Babbs, C. Neal, J. Mahoney, A. Saunders, R. Duncan, D. Tolia, R. Magu, C. Qopoto, H. Mahoa, and D. Natogga (1999). Geological-tectonic framework of Solomon Islands, SW Pacific: crustal accretion and growth within an intra-oceanic setting, *Tectonophysics* **301**, 35-60.

Phinney, E., P. Mann, M. Coffin, and T. Shipley (1999). Sequence stratigraphy, structure, and tectonics of the southwestern Ontong Java Plateau adjacent to the North Solomon trench and Solomon Islands arc, *J. Geophys. Res.* **104**, 20449-20466.

Phinney, E., P. Mann, M. Coffin, and T. Shipley (2004). Sequence stratigraphy, structural style, and age of deformation of the Malaita accretionary prism (Solomon arc-Ontong Java Plateau convergent zone), *Tectonophysics* **389**, 221-246.

Richards, S., R. Holm, and G. Barber (2011). When slabs collide: a tectonic assessment of deep earthquakes in the Tonga-Vanuatu region, *Geology* **39**, 787-790.

Taira, A., P. Mann, and R. Rahardiawan (2004). Incipient subduction of the Ontong Java Plateau along the North Solomon trench, *Tectonophysics* **389**, 247-266.

Taylor, B., A. Goodliffe, F. Martinez, and R. Hey (1995). Continental rifting and initial sea-floor spreading in the Woodlark basin, *Nature* **374**, 534-537.

Taylor, B., and N. Exon (1987). An investigation of ridge subduction in the Woodlark – Solomons region: introduction and overview, in *Geology and Offshore Resources of the Pacific Island Arcs – Solomon Islands and Bougainville, Papua New Guinea regions* Taylor, B. (Editor), Circum-Pacific Council for Energy and Mineral Resources, vol. 7. Earth Science Series, Houston, TX, 1-24.

Taylor, F. W., P. Mann, M. G. Bevis, R. L. Edwards, H. Cheng, K. B. Cutler, S. C. Gray, G. S. Burr, J. W. Beck, D. A. Phillips, G. Cabioch, and J. Recy (2005). Rapid forearc uplift and subsidence caused by impinging bathymetric features: Examples from the New Hebrides and Solomon arcs, *Tectonics* 24(6).

Taylor, F. W., R. W. Briggs, C. Frohlich, A. Brown, M. Hornbach, A. K. Papabatu, A. J. Meltzner, and D. Billy (2008). Rupture across arc segment and plate boundaries in the 1 April 2007 Solomons earthquake, *Nature Geoscience* **1**, 253-257.

Watts, A. B., and E. B. Burov (2003). Lithospheric strength and its relationship to the elastic and seismogenic layer thickness, *Earth Planet. Sci. Lett.* **213**(1-2), 113-131.

Wessel, P., Luis, J. F., Uieda, L., Scharroo, R., Wobbe, F., Smith, W. H. F., & Tian, D. (2019). The Generic Mapping Tools version 6. *Geochemistry, Geophysics, Geosystems, 20*, 5556–5564. https://doi.org/10.1029/2019GC008515.

Yan, C., and L. Kroenke (1993). A plate tectonic reconstruction of the SW Pacific, 0-100 Ma, in *Proceedings of the Ocean Drilling Program* Berger, T., Kroenke, L., Mayer, L., et al. (Editor), *Scientific Results* **130**, 697-709.

A Near-Vertical Slab Tear in the Southeastern Solomon Islands

C.-Y. Cheng[1*], H. Kuo-Chen[2], D. Brown[3], W.F. Sun[2], C.-S. Ku[4], Y.-T. Kuo[5], B.-S. Huang[4], and Y.-G. Chen[6]

[1]Department of Earth Sciences, National Central University, Taoyuan 320, Taiwan.
[2]Department of Geosciences, National Taiwan University, Taipei 10617, Taiwan.
[3]Geosciences Barcelona, CSIC, 08028 Barcelona, Spain.
[4]Institute of Earth Sciences, Academia Sinica, Taipei 11529, Taiwan.
[5]Department of Earth and Environmental Sciences, National Chung Cheng University, Chiayi 621301, Taiwan.
[6]Research Center for Environmental Changes, Academia Sinica, Taipei 11529, Taiwan.

Corresponding author: Ching-Yu Cheng (doll3219@gmail.com)

Abstract

The southeastern part of the Solomon Islands, a highly seismically active area in the southern Pacific, experienced two moderate earthquakes (Mw 6.3 and 6.0) on January 27th and 29th, 2020. The regional seismic network, operational since October 2018, recorded the entire foreshock-main-shock-aftershock sequence, allowing for a new 1D velocity model and relocation of events. Based on the spacial distribution of the foreshock-aftershock sequence, together with focal mechanism data from the Global CMT database, we suggest that there is a near-vertical slab tear at the southern end of the South Solomon subducting slab, abutting a zone of strike-slip faulting that links it to the Vanuatu subduction zone to form a Subduction-Transform Edge Propagator fault. Our new data also indicates that a seismic gap occurs at depths from 25 to 35 km within the southern part of the South Solomon slab.

Plain Language Summary

In October, 2018, a new regional seismic network was established in the southeastern Solomon Islands with six broadband seismic stations. In January, 2020, two large earthquakes occurred in the southeastern part of the Solomon Islands. The entire foreshock-aftershock sequence was recorded by the new network. Since a good 1D local velocity model is crucial for determining earthquake locations, we use the data set from this earthquake sequence to calculate a new 1D velocity model, and compare the earthquake hypocenter locations with those determined using the Preliminary Reference Earth Model (PREM). After the earthquakes are reliably located, we use the distribution of the foreshock-aftershock hypocenters to investigate the seismogenic structures in the southeastern South Solomon subduction zone and its link with the Vanuatu subduction zone. On the basis of these results, we suggest that there is a near-vertical slab tear along what we call the Makira – Santa Cruz transform forming what is termed a subduction-transform edge propagator (STEP) fault. We also observe a seismic gap in the South Solomon slab at depths from 25 to 35 km that is observed for the first time. With the current data set, the significance of this seismic gap is unclear.

1 Introduction

Extending for ~300 km in length, the link between the southeastern part of the South Solomon subduction zone and the northwestern Vanuatu subduction zone (Fig. 1) has been variably interpreted to be a subduction to strike-slip transition zone (e.g., Bilich et al., 2001) or has a continuation of the San Cristobal subduction zone but with a shortened slab length and a tear in the vicinity of the Santa Cruz Islands, where it interacts with the Vanuatu slab (e.g., Richards et al., 2011; Holm et al., 2016). Previous studies have mainly focused on the tectonic evolution of the Solomon Islands (e.g., Yan and Kroenke, 1993; Mann et al., 1998; Petterson et al., 1999; Mann and Taira, 2004; Holm et al., 2016), their geology (e.g., Mann et al., 1998; Taylor et al., 2005; Taylor et al., 2008; Chen et al., 2011), regional seismology (e.g., Cooper and Taylor, 1985; Mann and Taira, 2004; Chen et al., 2011), and crustal and upper mantle structures using ocean-bottom seismometer data (e.g., Mann et al., 1996; Phinney et al.,1999; Mann and Taira, 2004; Miura et al., 2004). To date, the subduction zone in the southeastern Solomon Islands and its possible linkage with the Vanuatu subduction zone has not been documented in detail due to sparse coverage of the area by seismic stations that could provide a data set with sufficient resolution for investigating the complex seismogenic, crustal, and upper mantle structures.

On January 27 and 29, 2020, two moderate earthquakes, Mw 6.3 and Mw 6.0, respectively, occurred in the southeastern Solomon Islands. The entire foreshock-main-shock-aftershock sequence was recorded by a new regional-scale seismic network that was set up in 2018. The earthquake sequence was located in the southeastern end of the South Solomon subduction zone, abutting the linkage zone with the Vanuatu subduction zone, providing a unique opportunity to look into the crustal and upper mantle structures of this tectonically complex region. The aim of this paper is to first derive a new, optimized local 1D P-wave velocity model utilizing the complete earthquake sequence, and compare the relocated hypocenters with those located using the Preliminary Reference Earth Model (PREM) (Dziewonski and Anderson, 1981). We then investigate the implications of the hypocenter locations for the structure of the southeastern part of the South Solomon subdction zone and its linkage with the Vanuatu subduction zone.

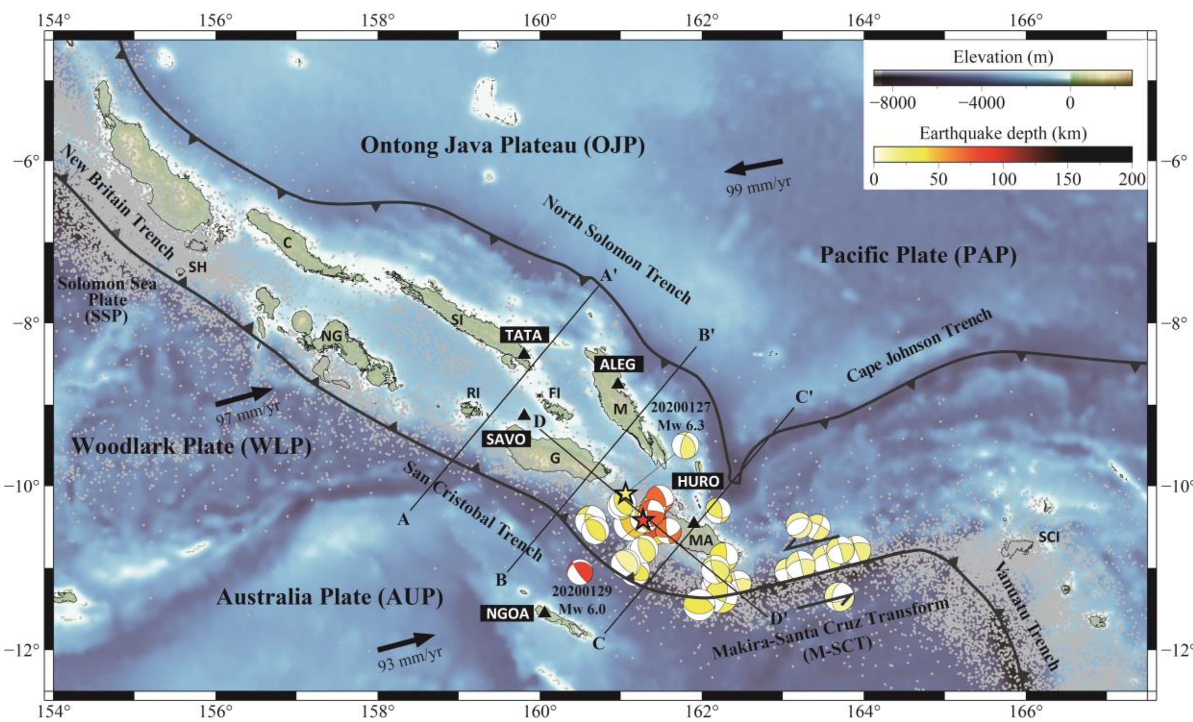

Figure 1. Topography, bathymetry, and regional tectonic setting of the Solomon Islands region. Arrows indicate direction and rate of plate motion of the Australia, Pacific, and Woodlark plates (NUVEL-1A, Demets et al., 1994); heavy lines with triangles represent subduction boundaries; black triangles are broadband seismic stations; two stars in the southeastern Solomon Islands

represent earthquakes occurred on January 27 and 29 from the Incorporated Research Institutions for Seismology (IRIS) catalog; focal mechanisms color-coded by depth are from GCMT; background seismicity are shown as gray dots and are compiled by the IRIS event catalog for the period 1971-2021; AA', BB', CC' and DD' are the cross sections in Figs. 2 and 4. SH, Shortland Islands; C, Choiseul; NG, New Georgia Island Group; SI, Santa Isabel; RI, Russell Islands; FI, Florida Islands; G, Guadalcanal; M, Malaita; MA, Makira; SCI, Santa Cruz Islands.

2 Tectonic setting

The Solomon Islands is located in a complex and active plate boundary where involving interactions among the Pacific plate (PAP), the Australian plate (AUP), and the associated microplates (i.e., the Woodlark plate and Solomon Sea plate) (Fig. 1) (e.g., Demets et al., 1990, 1994, 2010; Beavan et al., 2002; Miura et al., 2004; Phinney et al., 2004; Taira et al., 2004; Taylor et al., 2005, 2008; Argus et al., 2011; Newman et al., 2011). In the southern Solomon Islands, the Woodlark plate and the AUP subduct beneath the PAP forming the New Britain Trench, San Cristobal Trench and Vanuatu Trench (e.g., Taylor and Exon, 1987; Crook and Taylor, 1994; Taylor et al., 1995; Mann et al., 1998; Taylor et al., 2005). Using data from global seismic networks, previous seismological investigations suggest that active subduction now occurs primarily in the southeastern part of the South Solomon subduction zone, along the San Cristobal Trench (e.g., Cooper and Taylor, 1987; Mann et al., 1998; Chen et al., 2011). Furthermore, there is a waning, southwestward subduction of the Ontong Java Plateau along the North Solomon subduction zone, albeit with slight convergence (e.g., Taylor and Exon, 1987; Yan and Kroenke, 1993; Crook and Taylor, 1994; Mann et al., 1998; Petterson et al., 1999; Mann and Taira, 2004). The Solomon arc is considered a representative example of an island arc polarity reversal due to its unique opposing, double subduction zone setting.

The region around Makira Island and the Santa Cruz Islands (Fig. 1) contains two subduction-to-strike-slip transition (SSST) regions and a transform fault system linking the South Solomon and Vanuatu subduction zones (Bilich et al., 2001). In what follows, we call this the Makira-Santa Cruz transform (M-SCT). Although seismicity indicates a strike-slip motion along this zone (Fig. 1), some studies propose that the South Solomon slab may continues eastward along it, though significantly shortened, until it tears at the beginning of the Vanuatu subduction zone near the western end of the Santa Cruz Islands (Mann and Taira, 2004; Richards et al., 2011; Holm et al., 2016). The aim of this paper is to investigate the nature of the transition from the South Solomon subduction zone to the Makira-Santa Cruz transform.

3 Seismic network and data processing

In October, 2018, the Institute of Geological and Nuclear Sciences Limited (GNS), New Zealand, deployed six permanent seismic stations in different islets of the southeastern Solomon Islands (Fig. 1). To date, this seismic network has been maintained by the Ministry of Mines, Energy and Rural Electrification of the Solomon Islands Government. The instruments are equipped with broadband seismometer (Trillium 120PA; Nanometrics Inc., Canada) and 24-bits digital recorder (Q330S; Quanterra Inc., U.S.A.) with sampling rates of 100 Hz. Except for a timing problem with station LUES, most of the seismic waveforms recorded by the other five stations have good signal-to-noise ratios.

In this study, we processed two-month of continuous seismic waveforms from the GNS network, covering one month before and after the two January, 2020 events, encompassing the entire foreshock-aftershock earthquake sequence. In total, 730 earthquakes (Fig. 2a) were listed in the preliminary catalog, of which 651 were located within the seismic network. The data set is formatted with the daily miniSEED and we used the SeisAn Earthquake analysis software (SEISAN) to establish the event database (Havskov and Ottemoller, 1999). Most of the events occurred close to the seismic network, so we were able to extract numerous high-quality seismic waveforms to pick P- and S-wave arrivals, locate earthquakes and determine magnitudes. The earthquake catalog contains events detected by at least three stations and has more than one clear S-wave arrival to effectively constrain the depths of earthquakes. The interpolated 1D PREM velocity model was used as the reference model to locate earthquake hypocenters. We located earthquakes by the HYPOCENTER program (e.g., Lienert et al., 1986) and determined moment magnitude (M_w) by spectral analysis (e.g., Havskov and Ottemoller, 2010). Following this, we then used the program VELEST (Kissling, 1988, Kissling et al., 1994) to derive a new 1D velocity model, which produces the smallest possible uniform error for a set of seismic events with well-constrained locations. For this new velocity model, only events within the range of the seismic network with the root-mean-square error in arrival time from 0.5 to 1.0 s were used to invert a new

1D velocity model. In total, 389 events were selected for inversion to derive the preferred 1D model and then with it we relocated all 730 earthquakes to obtain the final catalog.

4 Results

4.1. New 1D velocity model

Because the initial velocity model (i.e. PREM) plays a crucial role in accurately locating earthquakes (Fig. 2b), it is important to determine the uncertainities involved. For the PREM velocity model, we calculate the standard error of the means in vertical (ERZ) and horizontal (ERH) as well as the root-mean-square error in arrival time of the 730 event locations in our data set to be 24.7 $\pm$ 19.15 km, 13.43 $\pm$ 10.8 km, and 0.61 $\pm$ 0.30 s, respectively. The moment magnitudes (M_w) determined in this study mostly range from 2.0 to 4.0 with a maximum of 4.9. For the new velocity model, the calculated root-mean-square error in arrival time is 0.66 $\pm$ 0.30 s. The distribution of the root-mean-square error in arrival times are more centralized after relocating and this may indicate the new model (Fig. 2b) is closer to the actual observed arrival times for this region. Furthermore, in comparison with PREM, the new velocity model has a higher velocity layer between 10 km and 25 km depth and slower velocity from 25-35 km depth (Fig. 2). At shallow depth (~10 km) the hypocenters relocated by the new velocity model are deeper and the cluster is more concentrated (Fig. 2c). At greater depth, the cluster becomes more concentrated.

4.2. South Solomon seismicity

In map view, our January-to-February 2020 data set reveals a significant rise in earthquake occurrences in the southeast. The majority of hypocenters form a single cluster, deepening northward near Makira Island, at the boundary between the South Solomon subduction zone and the Makira – Santa Cruz transform (Fig. 3). Other events form small clusters, or dispersed single events that extend from Santa Isabel Island and along the Makira - Santa Cruz transform. In the southeast, the South Solomon subduction zone hypocenters can be broadly divided into two clusters; a shallow cluster at roughly 0 to 25 km depth, and a second cluster between about 50 km and 100 km depth (Figs. 4a, b, and c). It is not clear from this data set whether the deeper events (>100 km) around Santa Isabel and Malaita islands (Fig. 3) are related to the South or North

Solomon subduction zones. Nevertheless, the hypocenters suggest that the South Solomon slab steepens significantly southeastward, from about 45^o near Santa Isabel Island to around 80^o at the transition to the Makira – Santa Cruz transform (Fig. 4). The area of shallow to moderately deep (ca. 100 km) earthquakes that form an open cluster between Santa Isabel and Malaita islands are clearly related to the North Solomon subduction zone (Fig. 4a). The amount of seismicity that can be attributed to the North Solomon subduction zone decreases significantly toward the southeast. In cross section, hypocenter locations suggest that the North Solomon slab dips about 60 ^{o}. In a NW-SE section, seismicity related to the North Solomon subduction zone decreases and shallows significantly at the Makira – Santa Cruz transform (Fig. 4d).

To gain further insight into the South Solomon subduction zone and its transition into the Makira – Santa Cruz transform, we also look at the background seismicity from 1971 to 2021 recorded in the IRIS catalog (Figs. 1 and 4). In these 50 years, ca. 5100 events were recorded in our study area. Overall, these show the same trends as our data set (Figs. 4e, f, g, and h), and this allows us to more confidently the interpret deeper (>100 km) events around Santa Isabel and Malaita islands to be related to the North Solomon subduction zone, whose slab appears to extend southward beneath that of the South Solomon subduction zone (Fig. 4e). The background seismicity also indicates that the South Solomon slab steepens towards the southeast. In a NW-SE section, it also shows that seismicity related to the North Solomon subduction zone decreases and shallows significantly at the Makira – Santa Cruz transform (Fig. 4h).

With only five active stations, it is not possible to determine focal mechanisms with our network. Nevertheless, focal mechanisms extracted from the Global CMT database shows the two January, 2020 main shocks to be oblique thrusts, similar to other events of MW >6.0 that occurred between 2000 and 2023 (Fig. 1). Along the Makira – Santa Cruz transform, focal mechanisms are nearly all strike-slip.

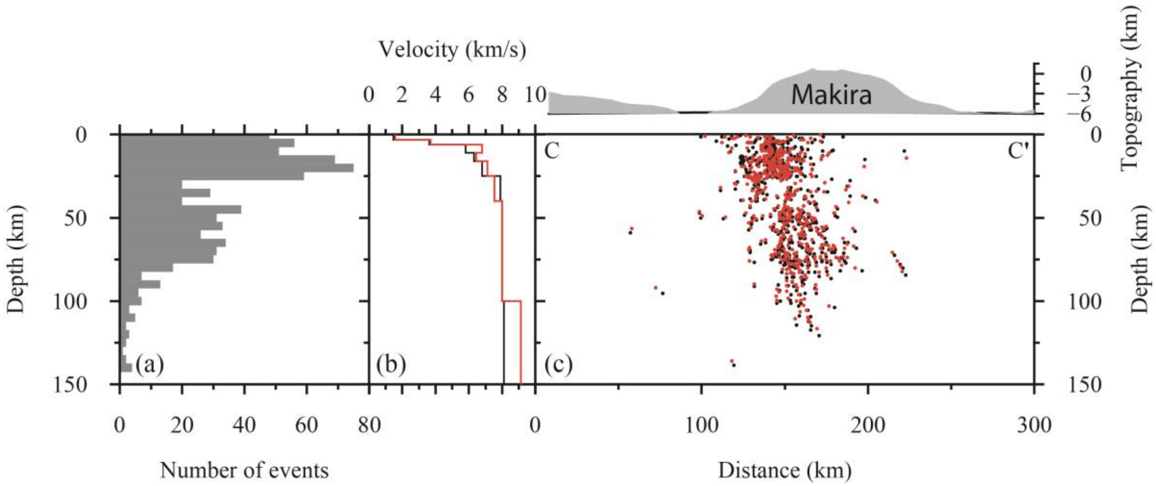

Figure 2. Seismic cluster of the southeastern Solomon Islands. (a) The event distribution in 5 km depth intervals. (b) The 1D interpolated PREM (black line) and the new velocity model (red line). Note the seismic gap between 25 km and 35 km depths. (c) CC’ cross section (in Fig. 4) with the seismic cluster located by the reference model (black dots) and relocated by the new velocity model (red dots).

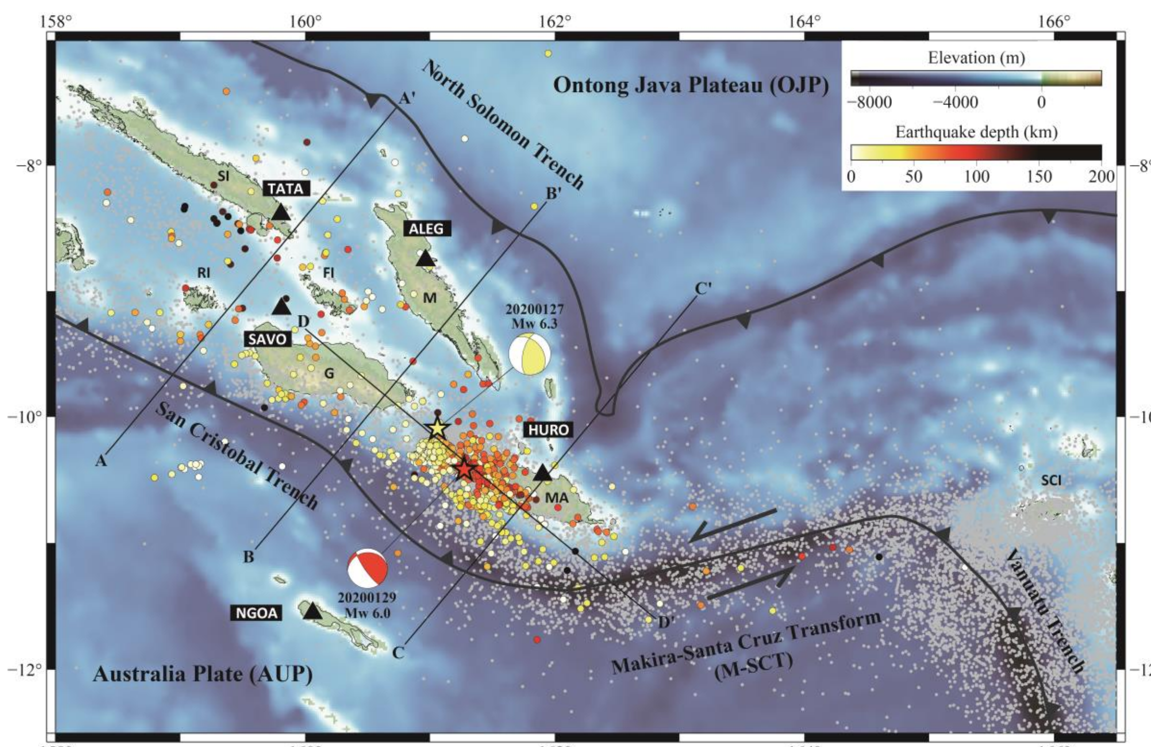

Figure 3. The spacial distribution of the foreshock-aftershock sequence. Topography, bathymetry, regional tectonic setting, and background seismicity are the same as in Fig. 1; circles color-coded by depth indicate foreshocks and aftershocks recorded by GNS seismic stations; stars are locations of the two January, 2020 main shocks; focal mechanisms of two main shocks are from GCMT and color-coded with depth.

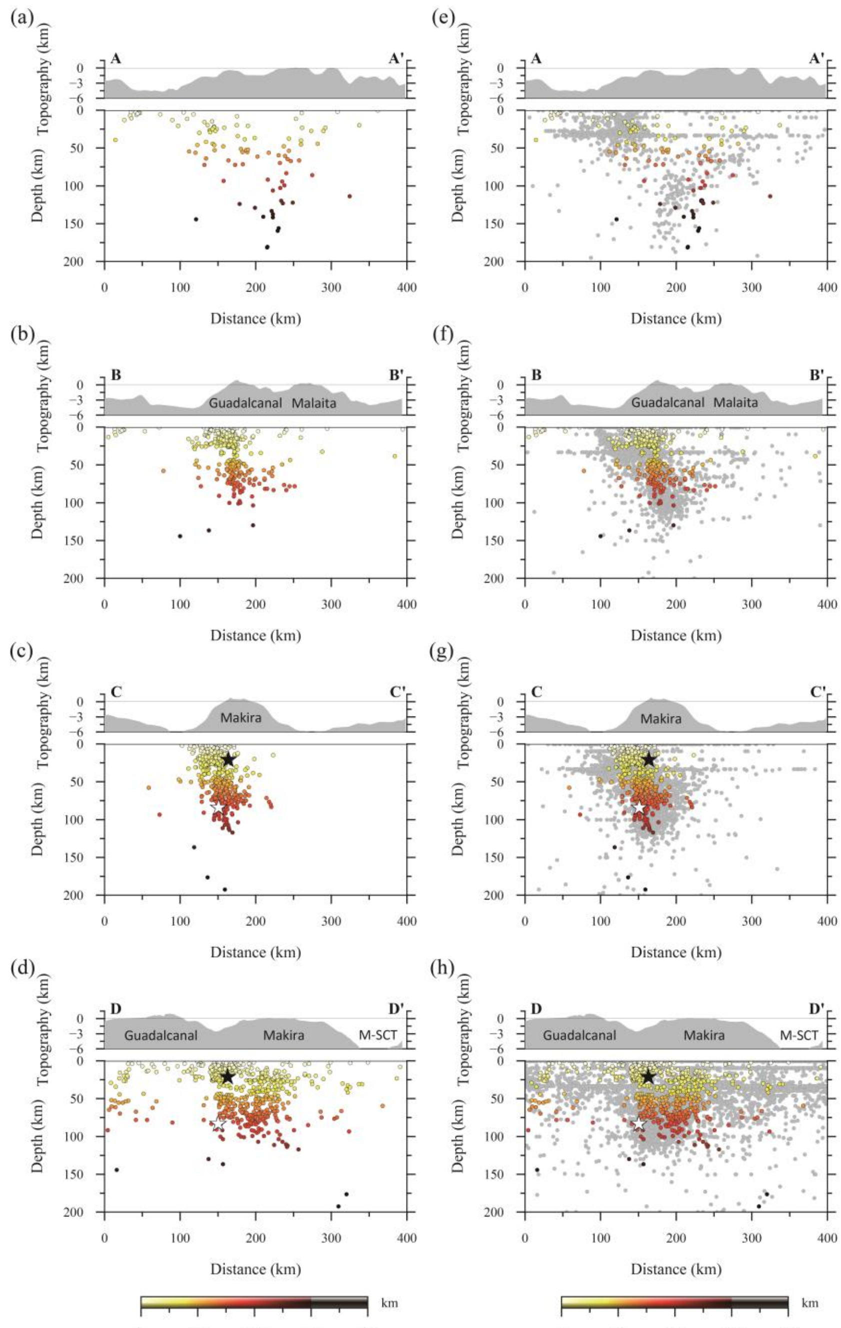

Figure 4. (a-d) Cross sections of earthquake hypocenters relocated by the new 1D velocity model. Circles color-coded by depth are foreshocks and aftershocks; black and white stars represent January 27 and 29 earthquakes in 2020 from IRIS event catalog; four 200-km-wide project lines are shown in Fig. 1. (e-h) Comparison of earthquake hypocenters located by the new 1D velocity model and background seismicity (gray dots). M-SCT = Makira - Santa Cruz transform.

5 Discussion

We used the complete foreshock-aftershock sequence of the January, 2020 earthquakes, recorded by the new seismic network, to calculate a more detailed 1D velocity model of the crust and mantle in the southeastern Solomon Islands. In particular, compared to PREM our velocity model shows a more varied and higher velocity layer between 10 km and 25 km depth, and a lower velocity from 25 km to 35 km depth where mantle velocities (ca. 8 km/s) are reached (Fig. 2). Recently, Ku et al. (2020) also calculated a low-velocity zone above the Moho in the Western Solomon Islands which they attribute to a lower crustal magma chamber (c.f. Dufek and Bergantz, 2005), but in our study area we unable to assign such a cause for the lower velocities found in our model. Nevertheless, because of the good coverage of the study area provided by the new network, the new velocity model provides better constraints of the quality of the earthquake location results and makes it possible to better locate local, small magnitude earthquakes, even at shallow depths.

STEP faults (or tearing) have been described from a number of subduction zones worldwide (e.g., Bilich et al., 2001; Grovers and Wortel, 2005). For example, Isacks et al. (1969) and Millen and Hamburger (1998) describe tearing along a zone of strike-slip faulting at the northern termination of the Tonga subduction zone, as do Molnar and Sykes (1969) and Clark et al. (2008) for the southern termination of the Lesser Antilles subduction zone. The model for STEP faults developed by Grovers and Wortel (2005), involves a subduction zone terminating at a strike-slip system that can range from 100’s to more than a 1000 km in length. Our study area presents a variation on this model in which the STEP fault links two subduction zones and we investigate the termination of the South Solomon subduction zone against the Makira – Santa Cruz transform, or the “convex” SSST of Bilich et al. (2001).

Our results show a steeply inclined seismogenic structure extending from the shallow subsurface to ~120 km depth beneath the island of Makira (Figs. 3 and 4). This structure, along with the background seismicity over the past 50 years, aligns within the SSST at the southwestern end of the Makira – Santa Cruz transform. On the basis of the southeastward truncation of the deep seismicity with predominantly thrust focal mechanisms against the Makira – Santa Cruz transform with predominately strike-slip focal mechanism, we suggest this area forms a subduction-transform edge propagator (STEP) fault (e.g., Grovers and Wortel, 2005) between the South Solomon subduction zone and the Vanuatu subduction zone (Fig. 5). Following the model of Govers and Wortel (2005), we suggest that the subducting South Solomon slab forms a steeply dipping seismogenic structure that terminates against a vertical tear in the lithosphere between the Australian Plate and the end of the Solomon Island arc (Fig. 5). Nevertheless, other authors (e.g., Mann and Taira, 2004; Richards et al., 2011; Holm et al., 2016) have different interpretations of the geometry and location of the southern termination of the South Solomon subduction zone, suggesting that the South Solomon slab continues eastward along the Makira – Santa Cruz transform to a slab tear at the northern termination of the Vanuatu subduction zone. We suggest, however, that geometry of the termination of the South Solomon slab at a STEP fault along the Makira – Santa Cruz transform fits better with the northward deepening seismicity with predominately thrust mechanisms around Makira Island abuting a northeast-trending zone of shallow seismicity with strike-slip mechanisms. In this interpretation, the Makira – Santa Cruz transform has been growing northeastward as the Vanuatu subduction zone advanced in that direction since about 4 Ma ago (e.g., Mann and Taira, 2004; Holm et al., 2016).

Our January-to-February, 2020 data set also suggest a seismic gap at 25-35 km depth within the cluster regardless of whether it is located in the PREM or the new velocity model (Fig. 4). Similar gaps in subduction-related seismicity have also been observed in seismic clusters in the Tonga Trench (Millen and Hamburger, 1998), Gibraltar (Buforn et al., 2004), the southeast Lesser Antilles Trench (Clark et al., 2008), and the northeast Lesser Antilles Trench (Meighan et al., 2013a). There are a few hypotheses regarding the cause of a gap in seismicity. For example, Clark et al. (2008) suggest that the gap images a weak, ductile, lower crustal layer separating a strong upper/middle crustal layer from a strong lithospheric mantle layer, which is interpreted as the "jelly sandwich" rheology (Chen and Molnar, 1983; Watts and Burov, 2003). In this model, Clark et al (2008) interprets the subducting slab to be detached from the buoyant South American plate along a near-vertical tear in the southeast corner of the Lesser Antilles Trench. Meighan et al. (2013b), propose that in the northeast Lesser Antilles subduction termination that the slab is overlain by an aseismic mantle wedge (e.g., van Keken et al., 2011), and therefore not directly contact with the overlying arc crust. In this model, the seismic gap is because there is shallow seismicity in the arc, no seismicity in the ductile mantle wedge, and then a vertical band of seismicity that crosses the entire slab. From our results, however, it is not clear what the exact reason for the gap in seismicity is. As a preliminary interpretation, we suggest that it could be related to a break in the end of slab that may be related to either drag along the transform and/or an early stage of slab breakoff.

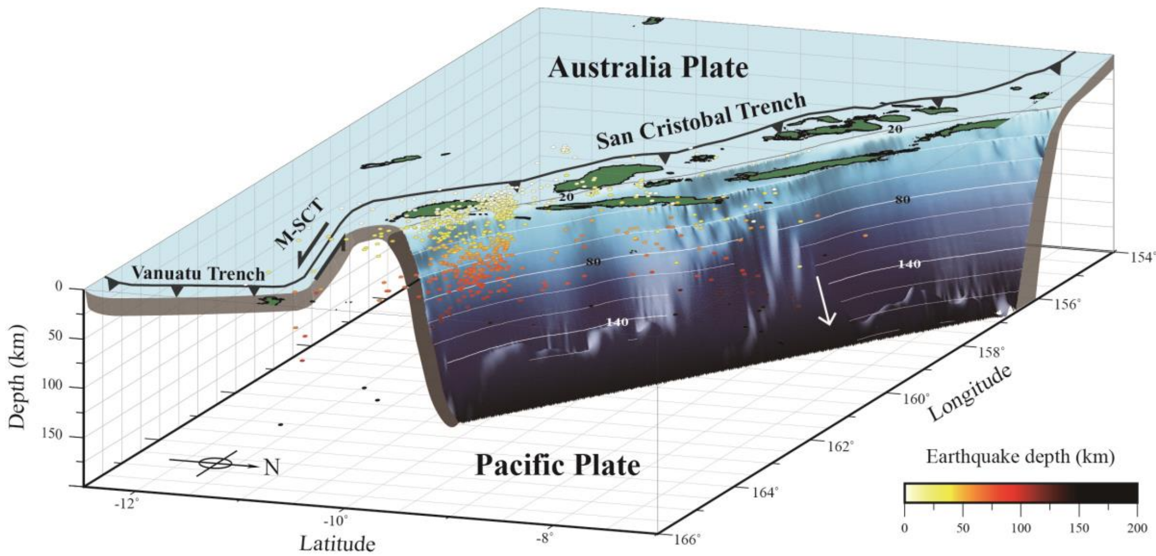

Figure 5. Three-dimensional visualization of the seismic cluster in the southeastern Solomon Islands viewed from northeast. Heavy lines with barbs represent subduction boundaries; solid contour lines are Slab2 – A Comprehensive Subduction Zone Geometry Model (Hayes et al., 2018), contoured every 20 km; earthquake hypocenters show near-vertical slab tear along the Makira – Santa Cruz transform.

6 Conclusions

In this study, we use a new seismic network that was established in the southeastern Solomon Islands in 2018 to provide better quality constraints on locating earthquakes in the area. We used a complete foreshock-aftershock sequence from two Jaunuary, 2020 earthquakes to calculate a new optimized local 1D velocity model and locate the hypocenters. The hypocenters define a steeply dipping earthquake cluster in the region between Makira and Guadalcannal, at the southeastern termination of the South Solomon subductions zone. This cluster terminates against the strike-slip Makira – Santa Cruz transform, which links the South Solomon and Vanuatu subduction zones. We suggest that the geometry and kinematics of this area is that of a thrust-dominated subduction zone termination against a strike-slip dominated subduction-transform edge propagator (STEP) fault. The gap observed in the Makira cluster at depths of 25-35 km may be indicative of a break in the South Solomon slab, although this is not clear from the data set. Futher investigations of the mechanism of slab tear and the cause of the seismic gap will be undertaken in the future.

Acknowledgements

This project is supported by Academic Sinica (Grant NO. AS-TP-110-M02). The assistance from Mr. Douglas Billy and Mr. Carlos Tatapu of Geological Survey Division, Solomon Islands Ministry of Mines, Energy and Rural Electrification (MMERE) are highly appreciated. Kuo-Chen and Brown wish to acknowledge visiting researcher grant NSTC 112-2811-M-002-006.

Open Research

The seismic data set used in this manuscript is available on https://tecdc.earth.sinica.edu.tw/WAV/2020SolomonIs/ (login with Email: solomon@earth.sinica.edu.tw and password: Islands2023).

Maps were created by using Generic Mapping Tools (GMT) version 6 (Wessel et al., 2019).

References

Argus, D. F., R. G. Gordon, and C. DeMets (2011). Geologically current motion of 56 plates relative to the no-net-rotation reference frame, *Geochemistry, Geophysics, Geosystems* **12**, no. 11.

Beavan, J. P., M. Tregoning, M. Bevis, and C. Meertens (2002). Motion and rigidity of the Pacific plate and implications for plate boundary deformation, *J. Geophy. Res.* **107**, 2261.

Bilich A., C. Frohlich, and P. Mann (2001). Global seismicity characteristics of subduction-to-strike-slip transitions, *J. Geophy. Res.* **106**, no. B9, 19433-19452.

Buforn E., M. Bezzeghoud, A. Udías, and C. Pro (2004). Seismic sources on the Iberia-African plate boundary and their tectonic implications, *Pure Appl. Geophys.* **161**, 623-646.

Chen M. C., C. Frohlich, F. W. Taylor, G. Burr, and A. Q. van Ufford (2011). Arc segmentation and seismicity in the Solomon Islands arc, SW Pacific, *Tectonophysics* **507**,47-69.

Chen, W. P., and P. Molnar (1983). Focal depths of intracontinental and intraplate earthquakes and their implications of the thermal and mechanical properties of the lithosphere, *J. Geophys. Res.* **88**, no. B5, 4183-4214.

Clark, S. A., M. Sobiesiak, C. A. Zelt, M. B. Magnani, M. S. Miller, M. J. Bezada, and A. Levander (2008). Identification and tectonic implications of a tear in the South American plate at the southern end of the Lesser Antilles, *Geochemistry, Geophysics, Geosystems* **9**, no. 11.

Cooper, P. A., and B. Taylor (1985). Polarity reversal in the Solomon Islands arc, *Nature* **314**, 428-430.

Cooper, P. A., and B. Taylor (1987). Seismotectonics of New Guinea: a model for arc reversal following arc-continent collision, *Tectonics* **6**, 53-67.

Crook, K., and B. Taylor, (1994). Structure and Quaternary tectonic history of the Woodlark triple junction region, Solomon Islands, *Marine Geophysical Researches* **16**, 65-89.

DeMets, C., R. G. Gordon, and D. F. Argus (2010). Geological current plate motions, *Geophys. J. Int.* **181**, 1-80.

DeMets, C., R. G. Gordon, D. F. Argus, and S. Stein (1990). Current plate motions, *Geophys. J. Int.* **101**,425-478.

DeMets, C., R. G. Gordon, D. F. Argus, and S. Stein (1994). Effect of recent revisions to the geomagnetic reversal time scale on estimates of current plate motions, *Geophys. Res. Lett.* **21**, 2191-2194.

Dufek, J., and G. W. Bergantz (2005). Lower crustal magma genesis and preservation: a stochastic framework for the evaluation of basalt-crust interaction. *J. Petrol.* **46**, 2167–2195.

Dziewonski, A. M., and D. L. Anderson (1981). Preliminary reference Earth model, *Physics of the Earth and Planetary Interiors* **25**(4), 297-356.

Forsyth, D. W. (1975). Fault plane solutions and tectonics of the South Atlantic and Scotia Sea, *J. Geophy. Res.* **80**, no. 11, 1429-1443.

Govers, R., and M. J. R. Wortel1 (2005). Lithosphere tearing at STEP faults: Response to edges of subduction zones, *Earth Planet. Sci. Lett.* **236**, 505-523.

Havskov, J., and L. Ottemoller (1999). SeisAn earthquake analysis software, *Seismol. Res. Lett.*

70, no. 5, 532-534.

Havskov, J., and L. Ottemoller (2010). *Routine Data Processing in Earthquake Seismology*, Springer, Dordrecht, The Netherlands.

Hayes, G. P., G. L. Moore, D. E. Portner, M. Hearne, H. Flamme, M. Furtney, and G. M. Smoczyk (2018). Slab2, a comprehensive subduction zone geometry model, Science **362**, 58-61.

Holm, R. J., G. Rosenbaum, S. W. Richards (2016). Post 8 Ma reconstruction of Papua New Guinea and Solomon Islands: Microplate tectonics in a convergent plate boundary setting, *Earth-Science Reviews* **156**, 66-81.

Isacks, B., L. R. Sykes, and J. Oliver (1969). Focal mechanisms of deep and shallow earthquakes in Tonga-Kermadec region and tectonics of island arcs, *Geol. Soc. Am. Bull.* **80**(8), 1443-1470.

Van Keken, B. E., B. R. Hacker, E. M. Syracuse, and G. A. Abers (2011). Subduction factory: 4. Depth-dependent flux of H_2O from subducting slabs worldwide, *J. Geophys. Res.* **116**, B01401.

Kissling, E. (1988). Geotomography with local earthquake data, *Reviews of Geophysics*. **26**, no. 4,659-698.

Kissling, E., W. L. Ellsworth, D. Eberhart-Phillips, and U. Kradolfer (1994). Initial reference model in local earthquake tomography, *J. Geophy. Res.* **99**, 19635-19646.

Ku, C. S., Y. T. Kuo, B. S. Huang, Y. G. Chen, and Y. M. Wu (2020). Seismic velocity structure beneath the Western Solomon Islands from the joint inversion of receiver functions and surface-wave dispersion curves, *Journal of Asian Earth Science* **195**, 104378.

Lienert, B. R. E., E. Berg, and L. N. Frazer (1986). Hypocenter: An earthquake location method using centered, scaled and adaptively least aquares, *Bull. Seismol. Soc. Am.* **76**, 771-783.

Mann, P., and A. Taira (2004). Global tectonic significance of the Solomon Islands and Ontong Java Plateau convergent zone, *Tectonophysics* **389**, 137-190.

Mann, P., F. W. Taylor, M. B. Lagoe, A. Quarles, and G. Burr (1998). Accelerating late Quaternary uplift of the New Georgia Islands Group (Solomon Island arc) in response to subduction of the recently active Woodlark spreading center and Coleman seamount, *Tectonophysics* **295**, 259-306

Mann, P., M. Coffin, T. Shipley, S. Cowley, E. Phinney, A. Teagan, K. Suyehiro, N. Takahashi, E. Araki, M. Shinohara, S. Miura, and L. Tivuru (1996). Researchers investigate fate of oceanic plateaus at subduction zones, *EOS Transactions American Geophysical Union* **77**, 282-283.

Meighan, H. E., J. Pulliam, U. S. ten Brink, and A. López (2013a). Seismic evidence for a slab tear at the Puerto Rico Trench, *J. Geophys. Res. Solid Earth* **118,** 2915-2923.

Meighan, H. E., U. ten Brink, and J. Pulliam (2013b). Slab tears and intermediate-depth seismicity, *Geophys. Res. Lett.* **40,** 4244-4248.

Millen, D. W., and M. W. Hamburger (1998). Seismological evidence for tearing of the Pacific plate at the termination of the Tonga subduction zone, *Geology* **26**, no. 7, 659-662.

Miura S., K. Suyehiro, M. Shinohara, N. Takahashi, E.Araki, and A. Taira (2004). Seismological structure and implications of collision between the Ontong Java Plateau and Solomon Island Arc from ocean bottom seismometer-airgun data, *Tectonophysics* **389**, 191-220.

Molnar, P., and L. R. Sykes (1969). Tectonics of the Caribbean and Middle America region from focal mechanisms and seismicity, *Geol. Soc. Amer. Bull*. **80**, 1639.

Newman, A. V., L. J. Feng, H. M. Fritz, Z. M. Lifton, N. Kalligeris, and Y. Wei (2011). The energetic 2010 M_W 7.1 Solomon Islands tsunami earthquake, *Geophys. J. Int.* **186**, 775-781.

Petterson, M., T. Babbs, C. Neal, J. Mahoney, A. Saunders, R. Duncan, D. Tolia, R. Magu, C. Qopoto, H. Mahoa, and D. Natogga (1999). Geological-tectonic framework of Solomon Islands, SW Pacific: crustal accretion and growth within an intra-oceanic setting, *Tectonophysics* **301**, 35-60.

Phinney, E., P. Mann, M. Coffin, and T. Shipley (1999). Sequence stratigraphy, structure, and tectonics of the southwestern Ontong Java Plateau adjacent to the North Solomon trench and Solomon Islands arc, *J. Geophys. Res.* **104**, 20449-20466.

Phinney, E., P. Mann, M. Coffin, and T. Shipley (2004). Sequence stratigraphy, structural style, and age of deformation of the Malaita accretionary prism (Solomon arc-Ontong Java Plateau convergent zone), *Tectonophysics* **389**, 221-246.

Richards, S., R. Holm, and G. Barber (2011). When slabs collide: a tectonic assessment of deep earthquakes in the Tonga-Vanuatu region, *Geology* **39**, 787-790.

Taira, A., P. Mann, and R. Rahardiawan (2004). Incipient subduction of the Ontong Java Plateau along the North Solomon trench, *Tectonophysics* **389**, 247-266.

Taylor, B., A. Goodliffe, F. Martinez, and R. Hey (1995). Continental rifting and initial sea-floor spreading in the Woodlark basin, *Nature* **374**, 534-537.

Taylor, B., and N. Exon (1987). An investigation of ridge subduction in the Woodlark – Solomons region: introduction and overview, in *Geology and Offshore Resources of the Pacific Island Arcs – Solomon Islands and Bougainville, Papua New Guinea regions* Taylor, B. (Editor), Circum-Pacific Council for Energy and Mineral Resources, vol. 7. Earth Science Series, Houston, TX, 1-24.

Taylor, F. W., P. Mann, M. G. Bevis, R. L. Edwards, H. Cheng, K. B. Cutler, S. C. Gray, G. S. Burr, J. W. Beck, D. A. Phillips, G. Cabioch, and J. Recy (2005). Rapid forearc uplift and subsidence caused by impinging bathymetric features: Examples from the New Hebrides and Solomon arcs, *Tectonics* 24(6).

Taylor, F. W., R. W. Briggs, C. Frohlich, A. Brown, M. Hornbach, A. K. Papabatu, A. J. Meltzner, and D. Billy (2008). Rupture across arc segment and plate boundaries in the 1 April 2007 Solomons earthquake, *Nature Geoscience* **1**, 253-257.

Watts, A. B., and E. B. Burov (2003). Lithospheric strength and its relationship to the elastic and seismogenic layer thickness, *Earth Planet. Sci. Lett.* **213**(1-2), 113-131.

Wessel, P., Luis, J. F., Uieda, L., Scharroo, R., Wobbe, F., Smith, W. H. F., & Tian, D. (2019). The Generic Mapping Tools version 6. *Geochemistry, Geophysics, Geosystems, 20*, 5556–5564. https://doi.org/10.1029/2019GC008515.

Yan, C., and L. Kroenke (1993). A plate tectonic reconstruction of the SW Pacific, 0-100 Ma, in *Proceedings of the Ocean Drilling Program* Berger, T., Kroenke, L., Mayer, L., et al. (Editor), *Scientific Results* **130**, 697-709.